Virologica Sinica (2019) 34:423–433
https://doi.org/10.1007/s12250-019-00113-4

www.virosin.org
www.springer.com/12250

RESEARCH ARTICLE

# *In Vitro* Infectious Risk Assessment of Heliothis virescens ascovirus 3j (HvAV-3j) toward Non-target Vertebrate Cells

Huan Yu[1,2] · Yi-Yi Ou-Yang[1,2] · Ni Li[1,2] · Madoka Nakai[3] · Guo-Hua Huang[1,2]

Received: 20 December 2018 / Accepted: 6 March 2019 / Published online: 29 April 2019


## Abstract

As specific pathogens of noctuid pests, including *Spodoptera exigua*, *S. litura*, *Helicoverpa armigera*, and *Mythimna separata*, ascoviruses are suitable for the development of bioinsecticides. In this study, the infectivity of Heliothis virescens ascovirus 3j (HvAV-3j) on insect and mammalian cells was evaluated. HvAV-3j infection induced drastic morphological changes in Sf9, HzAM1, SeFB, and HaFB cells, including swelling and detachment. Notably, the latter phenomena did not occur in HvAV-3j-inoculated mammalian cells (HEK293, 7402, HePG2, PK15, ST, and TM3). MTT assays indicated that HvAV-3j inhibited the growth of host insect cells from the 6th hpi, but no effects were detected in the HvAV-3j-inoculated mammalian cells. Furthermore, viral DNA replication, gene transcription, and protein expression were investigated, and the results consistently suggested that HvAV-3j viruses were not able to replicate their genomic DNA, transcribe, or express their proteins in the non-target vertebrate cells. The HvAV-3j genes were only transcribed and expressed in the four insect cell lines. These results indicated that HvAV-3j was infectious to cells derived from *S. frugiperda*, *S. exigua*, *H. armigera*, and *H. zea* but not to cells derived from human, pig, and mouse, suggesting that ascoviruses are safe to non-target vertebrate cells.

**Keywords** Infectious risk · Heliothis virescens ascovirus 3j (HvAV-3j) · Mammalian cells · Insect cells

## Introduction

Ascoviruses, belonging to the *Ascoviridae* family of insect-specific pathogens, contain a large circular double-stranded DNA (dsDNA) genome of 100–200 kb (Asgari *et al.* 2017), assembled in allantoid or rod-like virions (Federici 1983; Bigot *et al.* 1997; Cheng *et al.* 1999; Huang *et al.* 2012b; Wei *et al.* 2014; Huang *et al.* 2017; Arai *et al.* 2018). The size of the virions ranges from 200 to 400 nm. They are embedded in vesicles and accumulate in the host larval hemolymph (Federici *et al.* 1990; Federici and Govindarajan 1990). Ascoviruses can be divided into five major species: *Spodoptera frugiperda ascovirus 1* (including SfAV-1a and SfAV-1d), *Trichoplusia ni ascovirus 2* (including TnAV-2a and TnAV-2b), *Heliothis virescens ascovirus 3* (including HvAV-3a, HvAV-3e, HvAV-3h, HvAV-3i, and HvAV-3j), *Trichoplusia ni ascovirus 6* (including TnAV-6a and TnAV-6b, previously named as TnAV-2c and TnAV-2d respectively), and *Diadromus pulchellus toursvirus 1* (including DpTV-1a, previously named as DpAV-4a) (Carner and Hudson 1983; Hamm *et al.* 1986; Cheng *et al.* 2000; Asgari *et al.* 2007; Cheng *et al.* 2005; Huang *et al.* 2012b; Asgari *et al.* 2017; Huang *et al.* 2017; Arai *et al.* 2018; Liu *et al.* 2018; Chen *et al.* 2018, 2019). Heliothis virescens ascovirus 3j (HvAV-3j) is a recently reported isolate of *Heliothis virescens ascovirus 3a* from *Spodoptera litura* in Japan, and can be transmitted by the endoparasitoid *Meteorus pulchricornis* under laboratory conditions (Arai *et al.* 2018).

**Electronic supplementary material** The online version of this article (https://doi.org/10.1007/s12250-019-00113-4) contains supplementary material, which is available to authorized users.

✉ Madoka Nakai
madoka@cc.tuat.ac.jp

✉ Guo-Hua Huang
ghhuang@hunau.edu.cn

[1] Hunan Provincial Key Laboratory for Biology and Control of Plant Diseases and Insect Pests, Hunan Agricultural University, Changsha 410128, China

[2] College of Plant Protection, Hunan Agricultural University, Changsha 410128, China

[3] Tokyo University of Agriculture and Technology, Saiwai, Fuchu, Tokyo 183-8509, Japan

Laboratory data indicated that ascoviruses have the potential to develop into biopesticide owing to their high virulence to noctuid pests, such as *Spodoptera exigua*, *S. litura*, and *Helicoverpa armigera* (Federici 1982, 2009; Li *et al*. 2013, 2016; Yu *et al*. 2018b). Unlike the well-developed baculoviruses, the poor *per os* infectivity and the parasitoid-dependent transmission are the main possible constraints to the employment of ascoviruses for the development of bioinsecticides. In addition to their use as bioinsecticides, baculoviruses are widely employed as eukaryotic expression vectors and gene therapy vectors (Volkman and Goldsmith 1983; Carbonell *et al*. 1985), also due to their low environmental impact and lack of infectivity to non-target organisms (Arif 2005). As for ascoviruses, they have been only isolated from insect hosts, but infectivity to mammalian cells is not well documented.

In order to explore the infectivity of ascoviruses toward mammals, accurate *in vitro* detection was performed in four insect (Sf9, HzAM1, SeFB, and HaFB) and six mammalian cell lines (HEK293, 7402, HePG2, PK15, ST, and TM3), and the results were compared to those obtained using a baculovirus. This study provides insights into the evaluation of ascovirus-related risks to non-target organisms.

## Materials and Methods

### Cells and Viruses

Four insect and six mammalian cell lines were used to evaluate the infectivity of HvAV-3j. SeFB (IOZCAS-Spex-II-A) (Zhang *et al*. 2009) and HaFB cells were derived from the fat bodies of *S. exigua* and *H. armigera*, respectively. Sf9 and HzAM1 cells were obtained from ovary of *S. frugiperda* and *H. zea*, respectively. These four different insect cells were maintained in TMN-FH insect culture medium (Sigma, USA) with 10% FBS (GIBCO, USA) at 27 °C. HEK293 cells were derived from human renal epithelial cells; 7402 and HePG2 cell lines were derived from human lung cancer cells; PK15, ST, and TM3 cell lines were derived from porcine kidney epithelial, pig testis, and mouse testicular mesenchymal cells, respectively. These mammalian cells were cultured in DMEM medium (Hyclone, USA) with 10% FBS (GIMINI, USA) at 37 °C and 5% $CO_2$. HvAV-3j was stored at 4 °C in the hemolymph collected from the infected *S. exigua* larvae containing 0.5% phenylthiourea. A green florescence protein-encoding Autographa californica nucleopolyhedrovirus (AcMNPV-Egfp) was constructed and maintained in Sf9 cells and the budded viruses contained in the supernatant at multiplicity of infection (MOI) = 5 were used to inoculate different cultured cells for the following experiments.

### Cell Infection and Cell Viability Assays

The laboratory-maintained beet armyworm, *S. exigua*, was used for ascovirus infection and cultured on an artificial diet at 27 ± 1 °C and a 16/8 h (light/dark) photoperiod. To inoculate the ascovirus, the HvAV-3j-containing hemolymph mixture ($1.1 \times 10^{11}$ virion copies/mL) was prepared according to Li *et al*. (2016). HvAV-3j-containing *S. exigua* hemolymph was diluted 1000-fold with FBS-free TNM-FH medium. Diluted ascovirus-containing medium was sterilized by filtration with a 0.22-μm filter (Millipore, USA). The FBS was added to a final concentration of 10%. Hemolymph collected from *S. exigua* uninfected larvae was diluted and sterilized in the same way, and used as negative control (mock-infected control) in the following assays.

Cells were seeded in 6-well plates with a primary density of $10^5$ per well in 1 mL of medium and allowed to attach for 1 h. One milliliter of prepared HvAV-3j-containing medium, negative control medium, or AcMNPV-containing medium ($10^5$ $TCID_{50}$ $mL^{-1}$) were added into each well, as appropriate. To avoid repeated infection, the supernatant of each well was replaced with fresh culture medium after 1 h of infection, and this point was set as 0 h post-infection (hpi). At 0, 3, 6, 12, 24, 36, 48, 60, 72, 96, 120 and 168 hpi, the cell morphology was evaluated by reverse microscopy. Cells at the different time points post-virus inoculation were used to investigate the cell viability by the MTT method (Kim *et al*. 2007). To this end, cells were transferred into 96-well plates and, after allowing them to attach for 1 h, viruses were added. At different time points post-virus infection, the supernatant of each well was removed and 100 μL of 1 mg/mL 3-(4, 5-dimethyl-2-thiazolyl)-2,5-diphenyl-2-H-tetrazolium bromide (MTT) was added into each well. After a 4-h incubation, the culture medium in each well was replaced with 150 μL of DMSO. The absorbance at 490 nm was measured, and relative cell viability calculated as described by Kim *et al*. (2007).

At each time point, the differences in cell viability between mock-infected, HvAV-3j-infected, and AcMNPV-Egfp-infected cells were analyzed by two-way analysis of variance (ANOVA) using a least significant difference (LSD) test via SPSS (v16, SPSS Inc, Chicago, IL, USA). The general linear method (GLM) in SPSS was used to evaluate the differences in cell number and viability between the three treatments.

### Extraction of DNA, RNA, and Protein

Cells seeded in 6-well plates as above described were infected with HvAV-3j or AcMNPV-Egfp. At 0, 3, 6, 12, 24, 48, 72, 96, and 120 hpi, the cells were collected for DNA, RNA, and protein extraction. The DNA was extracted by using the TaKaRa MiniBEST Universal Genomic DNA Extraction Kit Ver.5.0 (TaKaRa, JPN), according to the manufacturer's instructions. The total RNA was extracted using TRI reagent (MRC, USA), according to the manufacturer's instructions, and the first-strand cDNA was obtained by reverse transcription with the RevertAid First Strand cDNA Synthesis Kit (Thermo Fisher Scientific) using 1.0 μg of total RNA as a template. The chloroform phase of each sample during the RNA extraction was used to obtain the total protein, according to the manufacturer's instructions for TRI reagent. For each time point, three replicate extractions of DNA, RNA, and protein samples were performed.

### Detection of Viral Genomic DNA Replication

The DNA replication curve of the recombinant viruses was investigated by qPCR as described by Li *et al*. (2016). The sequences of primers used for qPCR detection are shown in Supplementary Table S1. The GLM in SPSS 15.0 (SPSS Inc, Chicago, IL) was used to compare the differences in DNA replication between the different virus strains.

### Detection of Viral Gene Transcription

The cDNA synthesized from different cellular total RNAs, as described above, was used as template for PCR-based detection with the gene-specific primers shown in Supplementary Table S1. The major capsid protein gene (*mcp*, *orf56*) encodes the structural protein of HvAV-3j; the DNA polymerase (*Dpol*, *orf1*) and helicase genes (*helicase*, *orf133*) are genomic DNA synthesis-associated genes of HvAV-3j; the inhibitor of apoptosis protein 1 gene (*iap1*, *orf22*) and caspase-like gene (*casp*, *orf176*) are apoptosis-associated viral genes; the glycosyl transferase gene (*GTase*, *orf87*) is involved in carbohydrate metabolism. For AcMNPV detection, the *Dpol* (*orf65*), *38 K* (*orf98*), *gp64* (*orf128*), and *polyhedrin* (*polh*, *orf8*) were selected as the representatives of different functional genes. *Gapdh* was used as reference gene.

### Detection of Viral Protein Expression

Total proteins extracted from the different HvAV-3j-infected cells were analyzed by western blotting to evaluate the expression of the major capsid protein (MCP). The protein samples were separated by 12% SDS-PAGE and transferred to a nitrocellulose membrane. A polyclonal antibody against HvAV-3h MCP (1:3000; Yu *et al*. unpublished) and a monoclonal anti-β-actin antibody (1:4000; Proteintech, Cat No. 66005-1, CHN) were used as primary antibodies. The noctuid insect-specific GAPDH antibody (1:4000) was used as reference antibody (Yu *et al*. 2018a). Horseradish peroxidase (HRP)-conjugated goat anti-rabbit (1:5000) or HRP-conjugated goat anti-mouse lgG (1:5000) (Proteintech, CHN), were used as the secondary antibodies. The proteins were visualized by using Clarity™ Western ECL Substrate (Bio-Rad, USA).

## Results

### Morphological Changes Were Observed in HvAV-3j-inoculated Insect Cells But Not in HvAV-3j-inoculated Mammalian Cells

After exposure to HvAV-3j, significant morphological changes were observed in the four different tested insect cells. Aggregation and swelling of host cells were typical alterations caused by HvAV-3j infection (Fig. 1A, panel 1). The HvAV-3j-infected Sf9 cells acquired a round shape from the first day post-infection (dpi), and started to detach at 2 dpi; aberrant vesicles composed Sf9 cells were observed upon HvAV-3j infection at 2, 3, and 5 dpi; on the fifth day, the appearance of numerous spots indicated Sf9 cells destroyed by HvAV-3j infection. Swelling and rounding were also observed in HvAV-3j-infected HzAM1 cells (Fig. 1A, panel 2). Although typical vesicle-containing cells were also detected among infected HzAM1 cells, most of these cells were still intact at 5 dpi. SeFB cells suffered the most severe impact from HvAV-3j infection (Fig. 1A, panel 3). The mock-infected SeFB cells displayed a fibroblast-like appearance and maintained adherence to the surface of culture flasks. Upon HvAV-3j infection, above 60% of SeFB cells acquired a round shape and detached at 1 dpi; aggregated SeFB cells gradually broke into debris from 2 to 5 dpi; at 5 dpi, few swelled SeFB cells were still floating. HaFB cells were rarely destroyed by HvAV-3j infection, even at 5 dpi (Fig. 1A, panel 4). However, infected HaFB cells detached from the bottom of flasks and appeared granular from the first day post-infection. Thus, although infection by HvAV-3j induced swelling and floating in Sf9, HzAM1, SeFB, and HaFB cells, significantly different responses were observed in distinct cell lines.

In the AcMNPV-Egfp-infected Sf9 and SeFB cells, occlusion bodies typical of baculoviruses were found, and green fluorescence could be detected from the first day post-infection (Fig. 1B, panel 1, 3). In contrast, HzAM1

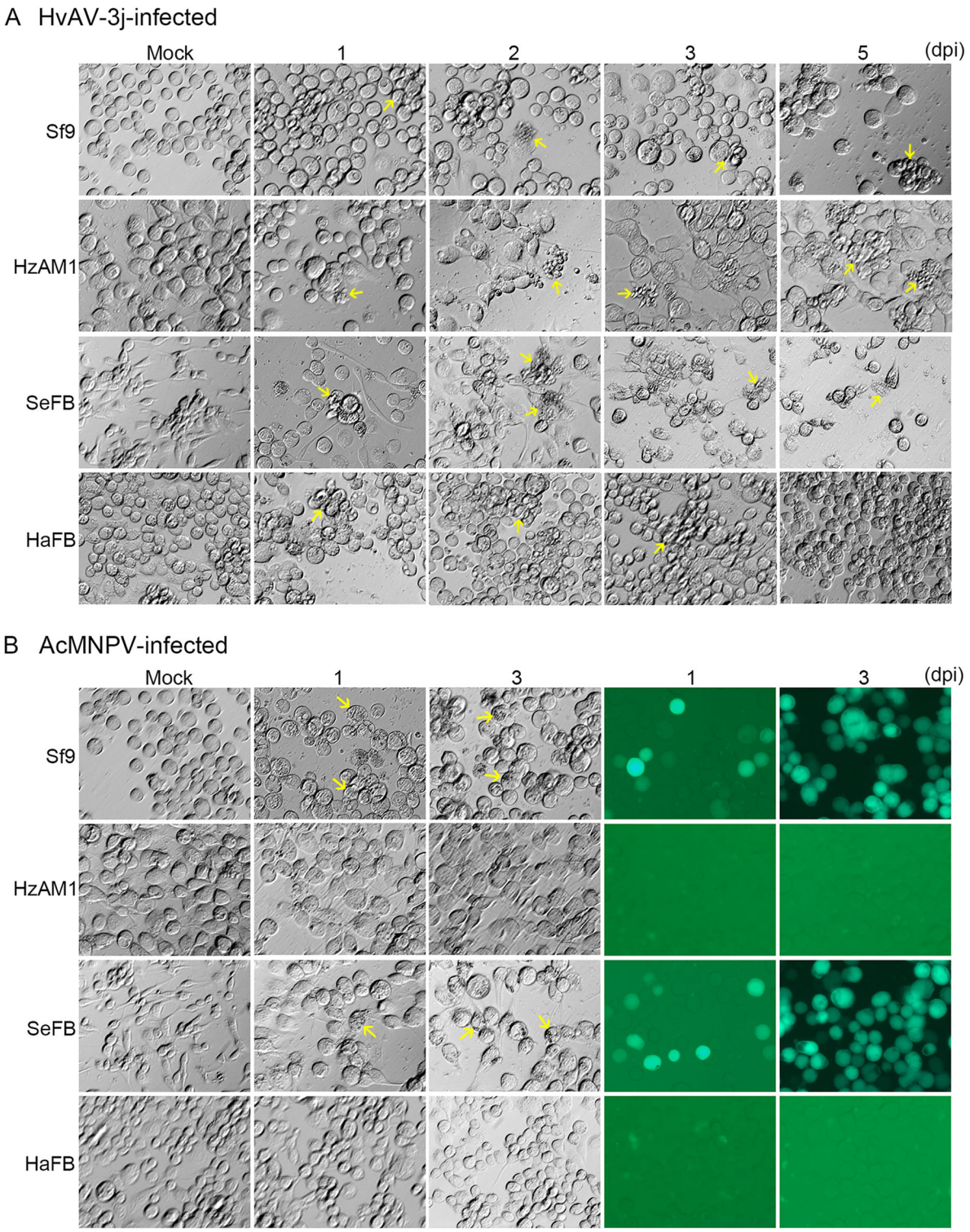


**Fig. 1** Microscopy analysis of virus-infected insect cell lines. Morphological changes in Sf9, HzAM1, SeFB, and HaFB cells inoculated with HvAV-3j (**A**) or AcMNPV-Egfp (**B**). Arrows in **A**: aggregated and malformed cells due to HvAV-3j inoculation; arrows in **B**: occlusion bodies induced by AcMNPV-Egfp. Magnification of all figures: 200×.

and HaFB cells grew normally after exposure to AcMNPV-Egfp, and no green fluorescence was detected from AcMNPV-Egfp-infected HzAM1 and HaFB cells (Fig. 1B, panel 2, 4). These results indicated that AcMNPV was infectious to Sf9 and SeFB cells, but not to HzAM1 and HaFB cells.

The effects of HvAV-3j and AcMNPV-Egfp infection were also explored in mammalian cells by monitoring cell morphology and EGFP expression (Fig. 2). Six mammalian cell lines were selected, *i.e.*, three human (HEK293, 7402, HePG2) and two pig cell lines (PK15, and ST), as well as a mouse cell line (TM3). All the selected cell lines grew normally in the presence of both HvAV-3j and AcMNPV-Egfp, and no green fluorescence could be detected. These results indicated that neither HvAV-3j nor AcMNPV can infect these six mammalian cells.

## Mammalian Cell Proliferation Was Not Affected by HvAV-3j Inoculation

To further characterize the impact of viral infection on cell proliferation, the relative cell viability was assessed by MTT assays. The infection by HvAV-3j nearly arrested Sf9, HzAM1, SeFB, and HaFB cell proliferation, and a significant inhibition of cell growth was observed at 12 hpi (Fig. 3). The proliferation indexes (PIs) of all HvAV-3j-infected insect cells drastically decreased from 6 to 12 hpi. In particular, PI decreased by 41.5% in Sf9 cells ($t = 16$, $df = 8$, $P < 0.0001$) and HzAM1 cells ($t = 8.068$, $df = 8$, $P < 0.0001$), by 39.8% in SeFB cells ($t = 3$, $df = 8$, $P = 0.0128$), and by 40.2% in HaFB cells ($t = 3.253$, $df = 8$, $P = 0.0117$). These results indicated that the HvAV-3j significantly inhibited the growth of host cells, and acute pathogenicity was observed between 6 and 12 hpi.

The MTT assays on AcMNPV-Egfp-infected insect cells were in close agreement with the results of the above described microscopy evaluation. According to the GLM analysis, no significant differences were observed between the PI of mock-infected and AcMNPV-Egfp infected HzAM1 ($F = 1.790$, $df = 11, 144$, $P = 0.082$) and HaFB ($F = 1.249$, $df = 11, 144$, $P = 0.283$) cells. On the other hand, AcMNPV infection significantly decreased the PI of Sf9 ($F = 85.28$, $df = 11, 144$, $P < 0.0001$) and SeFB ($F = 29.85$, $df = 11, 144$, $P < 0.0001$) cells, but this index was significantly higher compared to HvAV-3j-infected Sf9 ($F = 293.8$, $df = 11, 144$, $P < 0.0001$) and SeFB ($F = 245.6$, $df = 11, 144$, $P < 0.0001$) cells. These results

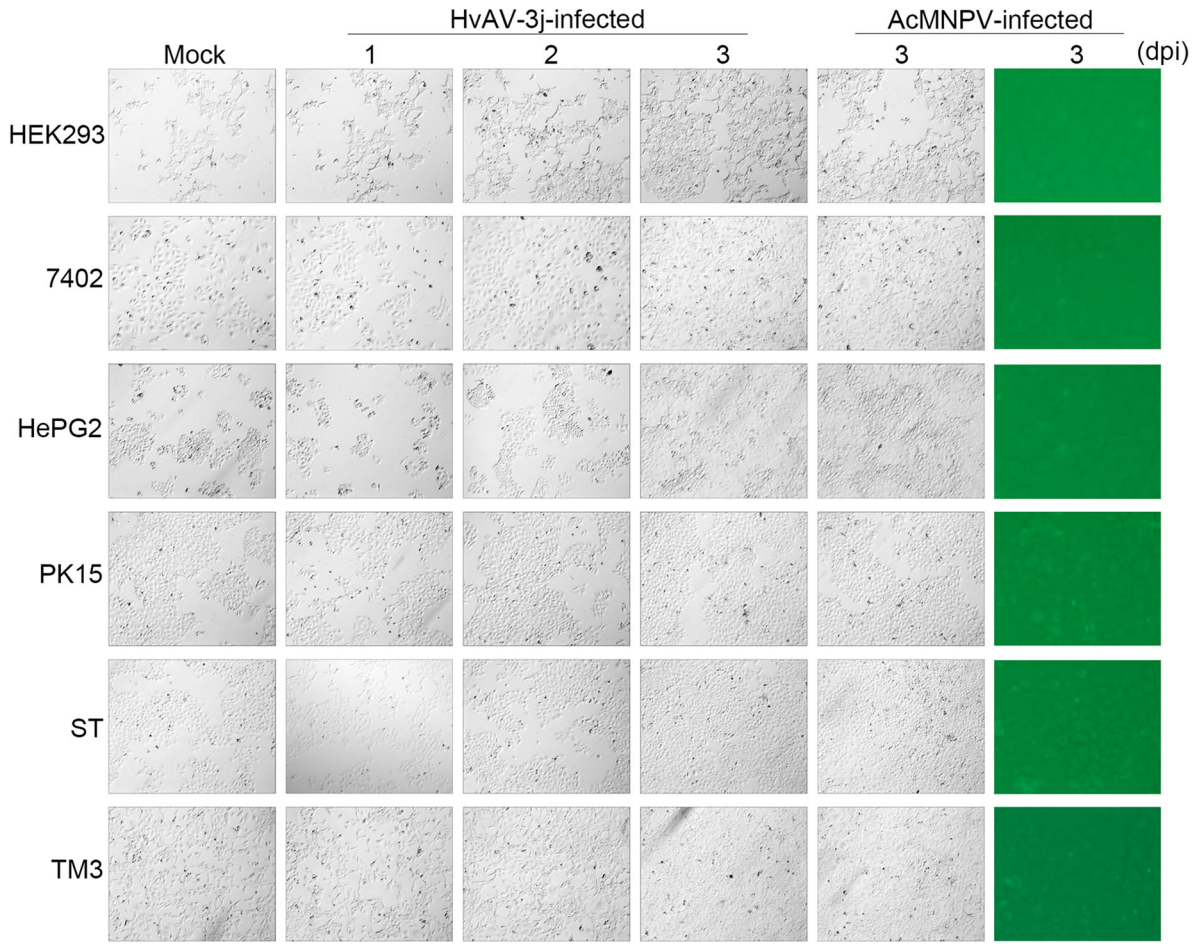


**Fig. 2** Microscopy analysis of virus-infected mammalian cell lines. Morphological appearance of HEK293, 7402, HePG2, PK15, ST, and TM3 cells inoculated with HvAV-3j or AcMNPV-Egfp. Magnification of all figures: 100×.

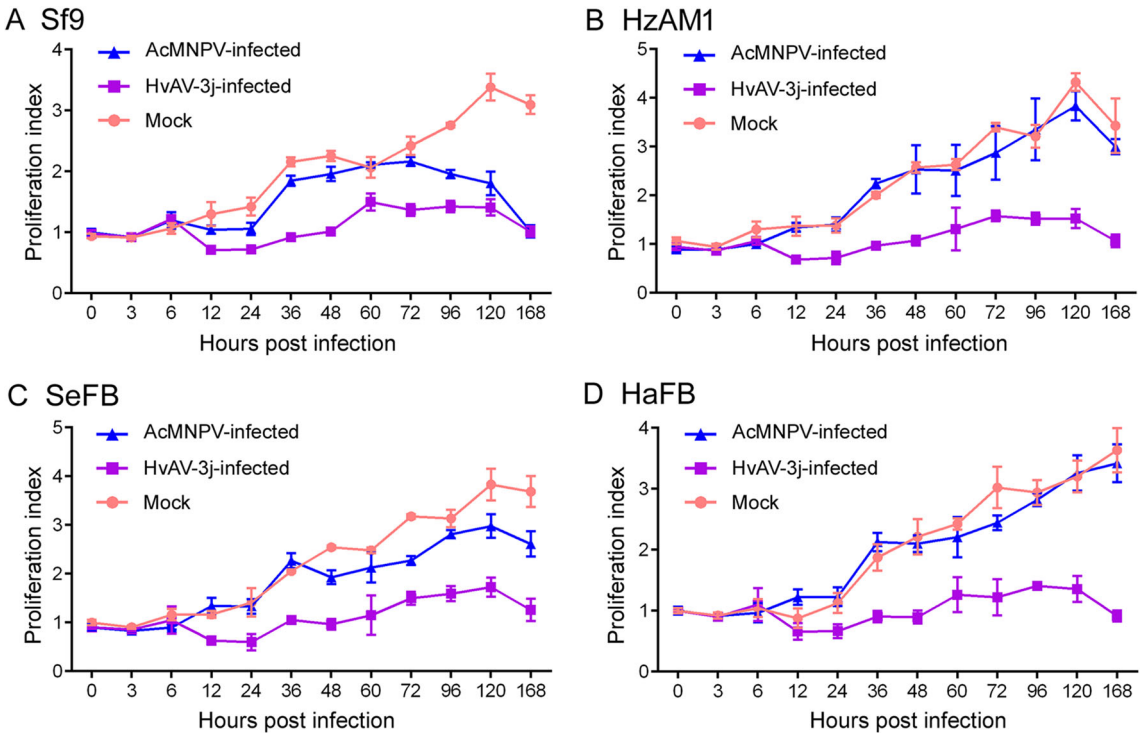


**Fig. 3** Insect cell viability after virus infection. Proliferation index measured by MTT assay after inoculation with HvAV-3j or AcMNPV-Egfp. **A** Sf9 cells. **B** HzAM1 cells. **C** SeFB cells. **D** HaFB cells.

indicated that AcMNPV had a lower impact on host cell growth (Sf9 and SeFB) compared to HvAV-3j.

MTT assays were also performed on HEK293, 7402, HePG2, PK15, ST, and TM3 cells to investigate the infectivity of HvAV-3j or AcMNPV on mammalian cells (Fig. 4). The results showed that in mammalian cells exposed to both HvAV-3j and AcMNPV-Egfp growth was comparable to that of mock-infected cells, in accordance with the above described microscopic observations.

## Determination of Viral DNA Replication in Different Cell Lines

In order to examine viral replication in the different cell lines, the HvAV-3j and AcMNPV-Egfp viral DNA content was analyzed by qPCR (Fig. 5). HvAV-3j viral DNA replication was similar in infected Sf9, HzAM1, SeFB, and HaFB cells (Fig. 5A). An interesting finding was that the HvAV-3j genomic DNA content increased at least one thousand-fold in the first 12 h after infection in all four insect cell lines examined, and in SeFB cells, HvAV-3j could produce millions of genome copies within 48 h after infection. Unlike HvAV-3j, AcMNPV-Egfp could only replicate in Sf9 and SeFB cells and finally yield ten thousand copies of its genome after 96 h of infection, corresponding to only 1% of HvAV-3j replication efficiency which was only 1% of HvAV-3j replication folds change (Fig. 5B). No viral DNA replication was detected from HvAV-3j- or AcMNPV-Egfp-infected HEK293, 7402, HePG2, PK15, ST, and TM3 cells, which indicated that neither HvAV-3j nor AcMNPV were infectious to mammalian cells.

## Viral Genes Were Not Transcribed in Mammalian Cell Lines

The transcription of viral genes was analyzed in HvAV-3j-infected insect cells to further explore viral infectivity. Among the HvAV-3j-encoded genes related to apoptosis, the genes for inhibitor of apoptosis protein 1 (*iap1*, *orf22*) and a caspase-like protein (*Casp*, *orf176*) started to be transcribed from 12 hpi. Transcription of the replication-associated HvAV-3j genes *helicase* (*orf133*) and *DNA polymerase* (*Dpol*, *orf1*) started at 12 hpi and continued until 96 hpi. The HvAV-3j gene for the structural major capsid protein (*mcp*, *orf56*) started to be transcribed at 24 hpi. Finally, transcription of the HvAV-3j gene for glycosyl transferase (*GTase*, *orf87*), implicated in carbohydrate metabolism, started at 12 hpi and continued until 96 hpi (Fig. 6A).

In the AcMNPV-Egfp infected insect cells, the *Dpol* (*orf65*), *38 K* (*orf98*), *gp64* (*orf128*), and *polyhedrin* (*polh*, *orf8*) transcripts were detected only in infected Sf9 and SeFB cells (Fig. 6B). *38k*, *gp64*, and *Dpol* transcription

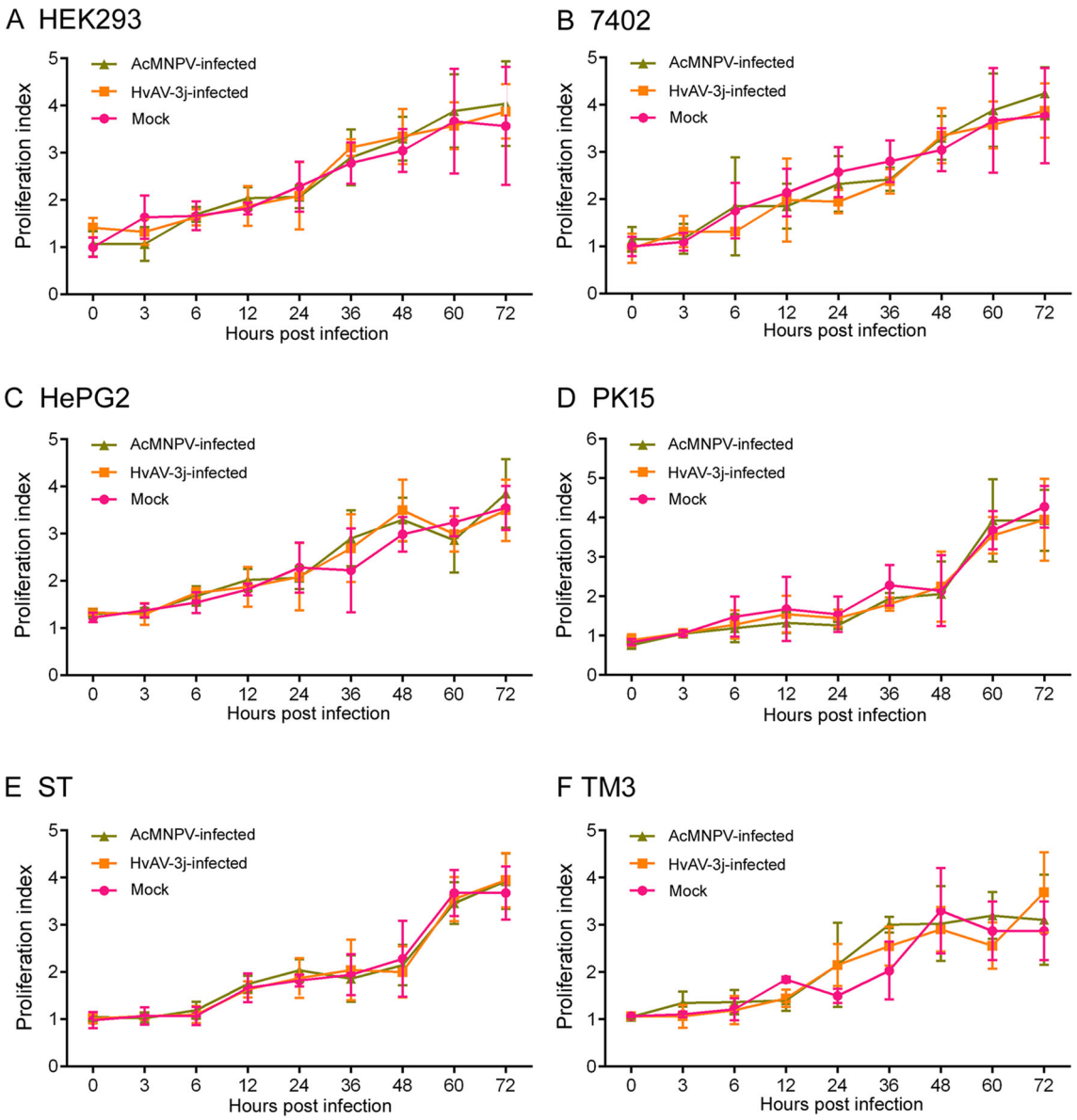


**Fig. 4** Mammalian cell viability after virus infection. Proliferation index measured by MTT assays in HEK293 (**A**), 7402 (**B**), HePG2 (**C**), PK15 (**D**), ST (**E**), and TM3 (**F**) after inoculation with HvAV-3j or AcMNPV-Egfp.

started at 12 hpi, whereas *polyhedrin* transcription was detected from 24 hpi (Fig. 6B). No viral transcripts were detected in HvAV-3j- or AcMNPV-Egfp-infected HEK293, 7402, HePG2, TM3, PK15 and ST cells, in line with the above described results.

### The Major Capsid Protein (MCP) of HvAV-3j Was Exclusively Detectable in Infected Insect Cells

Western blotting assays with a specific polyclonal antibody showed that MCP was expressed at 72 and 96 hpi in HvAV-3j-infected Sf9, HzAM1, SeFB, and HaFB cells (Fig. 7A, 7B), but no target bands were detected in HvAV-3j-infected HEK293, 7402, HePG2, PK15, ST, and TM3 cells (Fig. 7C, 7D). These results indicated that the HvAV-3j proteins were synthesized in Sf9, HzAM1, SeFB, and HaFB cells but not in the tested mammalian cells.

## Discussion

In this study, we assessed the risk of mammalian cell infection by HvAV-3j, based on cell morphology and viability, viral DNA replication, as well as transcription and protein expression of different viral genes. In order to compare HvAV-3j-induced effects on cell morphology

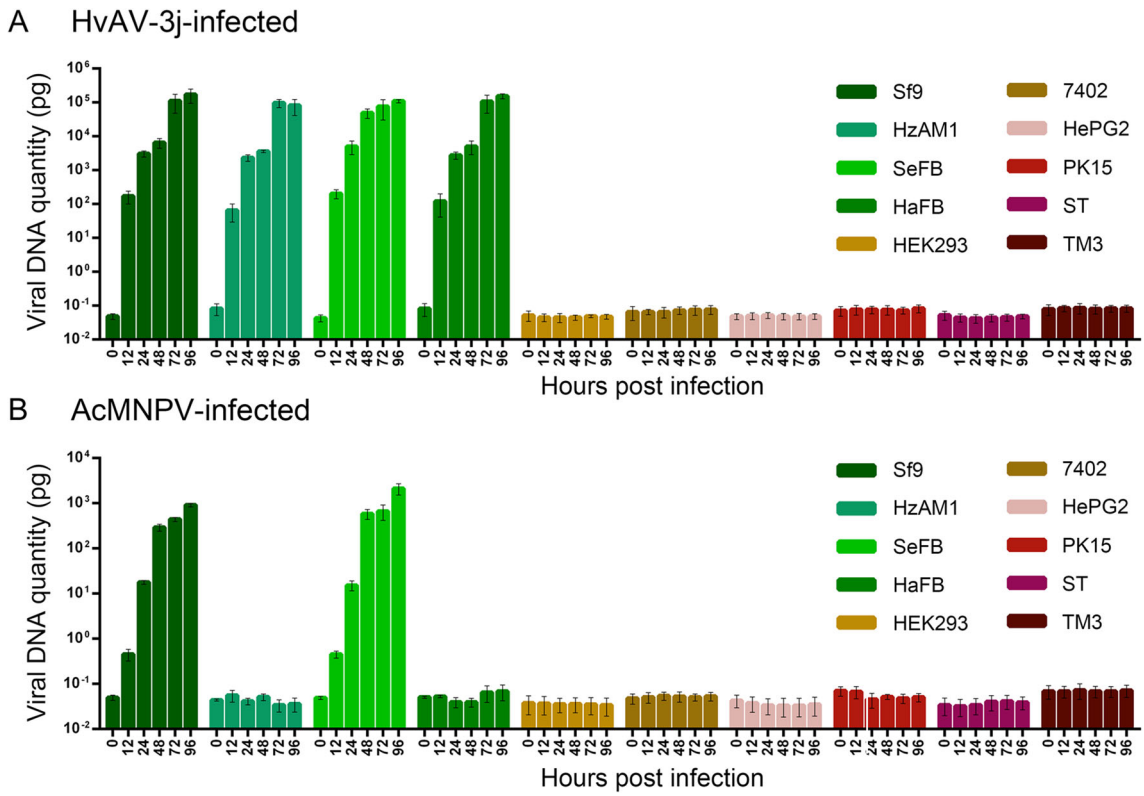


**Fig. 5** DNA replication of HvAV-3j (**A**) and AcMNPV-Egfp (**B**) viruses in Sf9, HzAM1, SeFB, HaFB, HEK293, 7402, HePG2, PK15, ST, and TM3 cells.

with those elicited by baculoviruses, a green fluorescence protein-expressing AcMNPV construct was generated and used as a control.

The infection of HvAV-3j caused the enlargement and release of insect cells from the flask on the first day post-infection (Fig. 1A). The HvAV-3j-infected Sf9 and SeFB cells eventually underwent lysis forming vesicles, but this destructive phenomenon was not observed in HzAM1 and HaFB cells, even at 7 dpi (data not shown). Similar events were previously observed with other ascoviruses, as exemplified by the effects of HvAV-3h on SeE1 and Sf9 cells (Huang *et al.* 2012a), of SfAV-1a on Sf21 cells (Bideshi *et al.* 2005), and of HvAV-3e on Sf9, Hz, and FB33 cells (Asgari 2006). These results indicated that infection by ascoviruses may lead to different changes in cell morphology in *Spodoptera* and *Helicoverpa*. It was reported that the HvAV-3h-infected *H. armigera* undergo an additional 20 days of larval life, compared to mock-infected larvae, corresponding to a 50% longer larval time than HvAV-3h-infected *S. exigua* and *S. litura* larvae (Li *et al.* 2013). Although it is not known which factors determine the time required for ascovirus-induced larval death, the speed of vesicle formation may play a critical role in this event.

The infection of HvAV-3j almost suppressed the proliferation of Sf9, HzAM1, SeFB, and HaFB cells, and the most significant decrease in proliferation took place between 6 and 12 hpi (Fig. 3). Acute pathogenicity of ascovirus was also reported in HvAV-3h-infected Sf9 and SeE1 cells (Huang *et al.* 2012a). Microscopic observation (Fig. 2) and cell proliferation assays (Fig. 4) indicated that HvAV-3j and AcMNPV did not exert cytotoxic or growth-inhibiting effects in human, pig, and mouse cells. Our results were similar to those previously obtained with baculoviruses, showing lack of infectivity toward mammalian cells, which was the precondition for their development into gene therapy vectors (Tjia *et al.* 1983; Volkman and Goldsmith 1983; Groener *et al.* 1984; Carbonell *et al.* 1985).

AcMNPV has a relatively broad host range as compared to other baculoviruses, and is infectious to several lepidopteran larvae. In this study, the constructed AcMNPV-Egfp was infectious to Sf9 and SeFB cells, but not to HzAM1 and HaFB cells, which was consistent with a previous study by Thiem (1997). qPCR quantification of viral DNA showed that AcMNPV-Egfp was able to replicate its genomic DNA hundreds of times after 24 hpi, and reached approximately ten thousand genome copies at 96 hpi (Fig. 5B). Studies examining baculoviral DNA

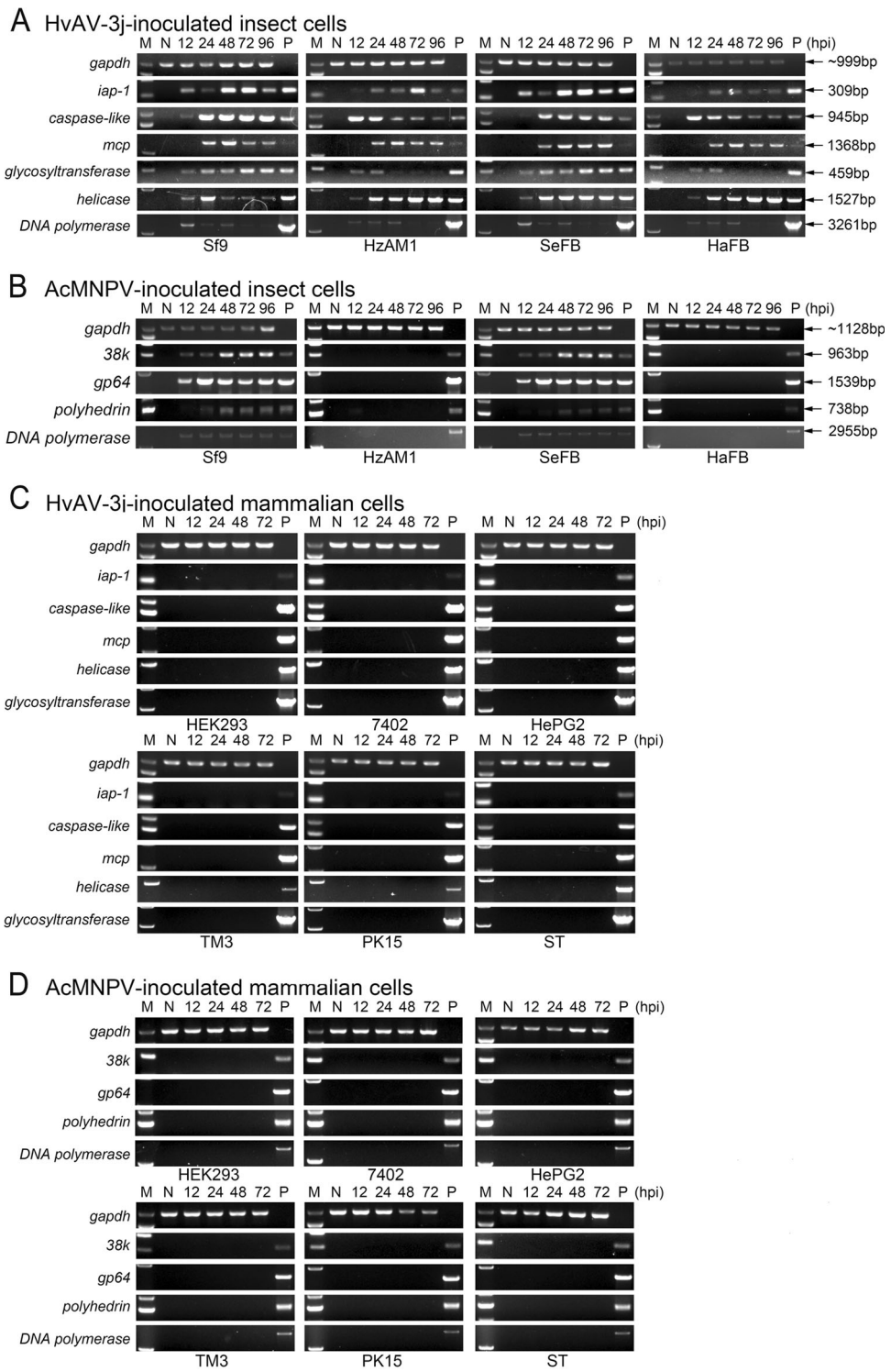


**Fig. 6** Transcription of selected viral genes in different cells. **A** Reverse transcription PCR (RT-PCR) of HvAV-3j-encoded iap-1, caspase-like, mcp, glycosyltransferase, helicase, and DNA polymerase in HvAV-3j-inoculated insect cells. **B** RT-PCR of AcMNPV-encoded 38k, gp64, polyhedrin, and DNA polymerase in AcMNPV-Egfp-inoculated insect cells. **C** RT-PCR of HvAV-3j-encoded iap-1, caspase-like, mcp, glycosyltransferase, helicase, and DNA polymerase in HvAV-3j-inoculated mammalian cells. **D** RT-PCR of AcMNPV-encoded 38k, gp64, polyhedrin, and DNA polymerase in AcMNPV-Egfp-inoculated mammalian cells. M: maker; N: negative control (PCR products from mock infected cellular cDNA); P: positive control (PCR products from vrial genomic DNA).

replication curves for AcMNPV or HearNPV reported a similar tendency (Wu *et al.* 2006; Tao *et al.* 2013; Zhu *et al.* 2013; Yu *et al.* 2015). HvAV-3j showed a more efficient DNA replication than AcMNPV-Egfp, producing thousands of DNA copies in 12 h, and millions of copies in 72 h (Fig. 5A). The higher replicative ability of ascoviruses is most likely related to their reproductive capacity, resulting in intracellular vesicle accumulation and causing the clear host larval hemolymph to change into a milky white suspension within the first 3 days post-infection (Govindarajan and Federici 1990). Interestingly, the growth rate of HvAV-3j was similar in all insect cells

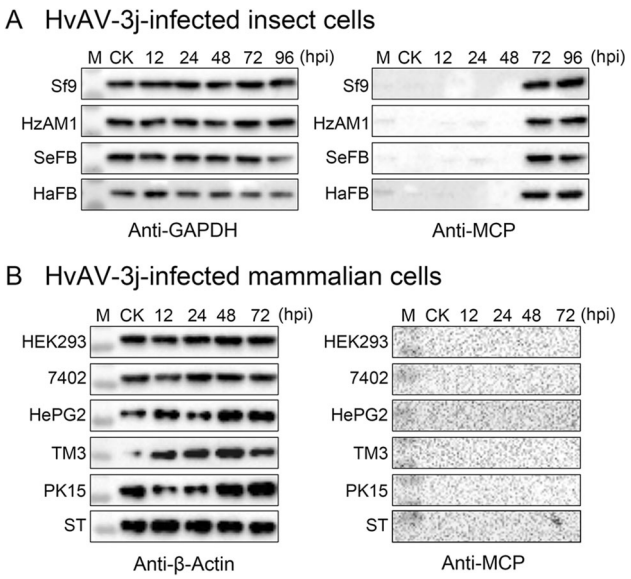


**Fig. 7** MCP expression detection in HvAV-3j infected cells. **A** Western blot of HvAV-3j-infected Sf9, HzAM1, SeFB, and HaFB cells with a prepared polyclonal antibody against MCP. A prepared polyclonal antibody against GAPDH was used to detect reference protein expression. **B** Western blot of HvAV-3j-infected HEK293, 7402, HePG2, TM3, PK15, and ST cells with a prepared polyclonal antibody against MCP. A commercially obtained monoclonal antibody against β-actin was used for detection of the reference protein. M: Marker; CK: Mock-infected cells.

examined in this study, including cells derived from *Heliothis* (HzAM1 and HaFB) or *Spodoptera* (Sf9 and SeFB). This suggests that the observed heterogeneous cytopathological effects were not due to a different viral permissiveness of the tested cell lines.

The analysis of transcription and expression of different viral protein was in total accordance with the results obtained from the analysis of viral DNA replication. HvAV-3j was not infectious to mammalian cells, as no viral protein was expressed in HvAV-3j- or AcMNPV-inoculated HEK293, 7402, HePG2, PK15, ST, and TM3 (Figs. 6, 7).

We demonstrated that ascovirus could not infect mammalian cells *in vitro*, and that the infection by HvAV-3j caused distinct cytopathological alterations in *Spodoptera* and *Helicoverpa* cells. Moreover, HvAV-3j infection resulted in early pathogenicity to host insect cells, as assessed by rapid DNA replication and significant decline in cell viability from 6 to 12 hpi. Finally, ascovirus exhibited a more efficient DNA replication as compared to baculovirus. The latter finding evokes the possibility of using ascoviruses as protein expression vectors. However, additional experiments are needed to in-depth characterize the mechanistic basis for the efficient DNA replication of ascovirus. In conclusion, our results indicated that ascoviruses are safe to non-target vertebrate cells, supporting their potential use for the development of biocontrol agents and gene therapy vectors.

**Acknowledgements** The authors thank Dr. Zhi-Hong Hu (Wuhan Institute of Virology, Chinese Academy of Sciences) for generously providing HzAM1, Sf9 cells and *E. coli* strain of DH10Bac; Dr. Qi-Lian Qin (Institute of Zoology, Chinese Academy of Sciences) for generously providing SeFB cells; Dr. Jian-Hong Li (College of Plant Science & Technology, Huazhong Agricultural University) for kindly providing HaFB cells; Dr. Si Qin (College of Food Science and Technology, Hunan Agriculture University) kindly giving HePG2 cells; Dr. Yun Liu (Zunyi Medical University) generously providing 7402 cells; Dr. Zhong Ding (College of Plant Protection, Hunan Agriculture University) generously providing HEK293 cells; Dr. Qing Yang (College of Veterinary Medicine, Hunan Agriculture University) generously providing PK15, ST, and TM3 cells. This work was supported by the National Natural Science Foundation of China (31700141, 31872027) and the grant of Chinese Post-doctoral special funding (2018T110832) and Program to supporting research activities of female researchers in Ministry of education, culture, sports, science and technology-Japan.

**Author Contributions** HY, MN and GHH contributed to the study design. HY, YYOY and NL performed the experiments. HY, MN and GHH contributed reagents. HY and YYOY analyzed the data. HY, YYOY, MN and GHH wrote the manuscript. All authors read and approved the final manuscript.

## Compliance with Ethical Standards

**Conflict of interest** The authors declared no competing financial interests in this paper.

**Animal and Human Rights Statement** This article does not contain any studies with human or animal subjects performed by any of the authors.

## References

Arai E, Ishii K, Ishii H, Sagawa S, Makiyama N, Mizutani T, Omatsu T, Katayama Y, Kunimi Y, Inoue MN, Nakai M (2018) An ascovirus isolated from *Spodoptera litura* (Noctuidae: Lepidoptera) transmitted by the generalist endoparasitoid *Meteorus pulchrcornis* (Braconidae: Hymenoptera). J Gen Virol 99:574–584

Arif BM (2005) A brief journey with insect viruses with emphasis on baculoviruses. J Invertebr Pathol 89:39–45

Asgari S (2006) Replication of *Heliothis virescens ascovirus* in insect cell lines. Arch Virol 151:1689–1699

Asgari S, Davis J, Wood D, Wilson P, McGrath A (2007) Sequence and organization of the *Heliothis virescens ascovirus* genome. J Gen Virol 88:1120–1132

Asgari S, Bideshi DK, Bigot Y, Federici BA, Cheng X (2017) ICTV report consortium, ICTV virus taxonomy profile: *Ascoviridae*. J Gen Virol 98:4–5

Bideshi DK, Tan KP, Bigot Y, Federici BA (2005) A viral caspase contributes to modified apoptosis for virus transmission. Gene Dev 19:1416–1421

Bigot Y, Rabouille A, Sizaret PY, Hamelin MH, Periquet G (1997) Particle and genomic characteristics of a new member of the

*Ascoviridae*: Diadromus pulchellus ascovirus. J Gen Virol 78:1139–1147

Carbonell LF, Klowden MJ, Miller LK (1985) Baculovirus mediated expression of bacterial genes in dipteran and mammalian cells. J Virol 56:153–160

Carner GR, Hudson JS (1983) Histopathology of virus-like particles in *Heliothis* spp. J Invertebr Pathol 41:238–249

Chen ZS, Hou DH, Cheng XW, Wang X, Huang GH (2018) Genomic analysis of a novel isolate Heliothis virescens ascovirus 3i (HvAV-3i) and identification of ascoviral repeat ORFs (aros). Arch Virol 163:2849–2853

Chen ZS, Cheng XW, Wang X, Hou DH, Huang GH (2019) Proteomic analysis of the Heliothis virescens ascovirus 3i (HvAV-3i) virion. J Gen Virol 100:301–307

Cheng XW, Carner GR, Brown TM (1999) Circular configuration of the genome of ascoviruses. J Gen Virol 80:1537–1540

Cheng XW, Carner GR, Arif BM (2000) A new ascovirus from *Spodoptera exigua* and its relatedness to the isolate from *Spodoptera frugiperda*. J Gen Virol 81:3083–3092

Cheng XW, Wang LH, Carner GR, Arif BM (2005) Characterization of three ascovirus isolates from cotton insects. J Invertebr Pathol 89:193–202

Federici BA (1982) A new type of insect pathogen in larvae of the clover cutworm, *Scotogramma trifolii*. J Invertebr Pathol 40:41–54

Federici BA (1983) Enveloped double-stranded DNA insect virus with novel structure and cytopathology. Proc Natl Acad Sci USA 80:7664–7668

Federici BA, Govindarajan R (1990) Comparative histopathology larval of three ascovirus noctuids isolates in larval noctuids. J Invertebr Pathol 56:300–311

Federici BA, Vlak JM, Hamm JJ (1990) Comparative study of virion structure, protein composition and genomic DNA of three ascovirus isolates. J Gen Virol 71:1661–1668

Federici BA, Bideshi DK, Tan Y, Spears T, Bigot Y (2009) Ascoviruses: superb manipulators of apoptosis for viral replication and transmission. Curr Top Microbiol 328:171–196

Govindarajan R, Federici BA (1990) Ascovirus infectivity and effects of infection on the growth and development of noctuid larvae. J Invertebr Pathol 56:291–299

Groener A, Granados RR, Burand JP (1984) Interaction of *Autographa californica* nuclear polyhedrosis virus with two nonpermissive cell lines. Intervirology 21:203–209

Hamm JJ, Pair SD, Marti OG (1986) Incidence and host range of a new ascovirus isolated from fall armyworm, *Spodoptera frugiperda* (Lepidoptera: Noctuidae). Fla Entomol 69:524–531

Huang GH, Garretson TA, Cheng XH, Holztrager MS, Li SJ, Wang X, Cheng XW (2012a) Phylogenetic position and replication kinetics of *Heliothis virescens ascovirus* 3 h (HvAV-3h) isolated from *Spodoptera exigua*. PLoS ONE 7:e40225

Huang GH, Wang YS, Wang X, Garretson TA, Dai LY, Zhang CX, Cheng XW (2012b) Genomic sequence of *Heliothis virescens ascovirus* 3 g isolated from *Spodoptera exigua*. J Virol 86:12467–12468

Huang GH, Hou DH, Wang M, Chen XW, Hu Z (2017) Genome analysis of Helithis virescens ascovirus 3h isolated from China. Virol Sin 32:147–154

Kim E, Jeon IS, Kim JW, Kim J, Jung HS, Lee SJ (2007) An MTT-based method for quantification of periodontal ligament cell viability. Oral Dis 13:495–499

Li SJ, Wang X, Zhou ZS, Zhu J, Hu J, Zhao YP, Zhou GW, Huang GH (2013) A comparison of growth and development of three major agricultural insect pests infected with *Heliothis virescens ascovirus* 3 h (HvAV-3h). PLoS ONE 8:e85704

Li SJ, Hopkins RJ, Zhao YP, Zhang YX, Hu J, Chen XY, Xu Z, Huang GH (2016) Imperfection works: survival, transmission and persistence in the system of Helithis virescens ascovirus 3h (HvAV-3h), *Microplitis similis* and *Spodoptera exigua*. Sci Rep 16:21296

Liu YY, Xian WF, Xue J, Wei YL, Cheng XW, Wang X (2018) Complete Genome Sequence of a Renamed Isolate, Trichoplusia ni ascovirus 6b, from the United States. Genome Announc 6:e00148–18

Tao XY, Choi JY, Kim WJ, Lee JH, Liu Q, Kim SE, An SB, Lee SH, Woo SD, Jin BR, Je YH (2013) The *Autographa californica* multiple nucleopolyhedrovirus ORF78 is essential for budded virus production and general occlusion body formation. J Virol 87:8441–8450

Thiem SM (1997) Prospects for altering host range for baculovirus bioinsecticides. Curr Opin Biotechnol 8:317–322

Tjia ST, Altenschildesche GM, Doerfler W (1983) *Autographa californica* nuclear polyhedrosis virus (AcNPV) DNA does not persist in mass cultures of mammalian cells. Virology 125:107–117

Volkman LE, Goldsmith PA (1983) In vitro survey of *Autographa californica* nuclear polyhedrosis virus interaction with nontarget vertebrate host cells. Appl Environ Microbiol 45:1085–1093

Wei YL, Hu J, Li SJ, Chen ZS, Cheng XW, Huang GH (2014) Genome sequence and organization analysis of Helithis virecens ascovirus 3f isolated form a Helicoverpa zea larva. J Invertebr Pathol 122:40–43

Wu WB, Lin TH, Pan LJ, Yu M, Li ZF, Pang Y, Yang K (2006) *Autographa californica* multiple nucleopolyhedrovirus nucleocapsid assembly is interrupted upon deletion of the 38 K gene. J Virol 80:11475–11485

Yu H, Xu J, Liu Q, Liu TX, Wang D (2015) Ha83, a chitin binding domain encoding gene, is important to *Helicoverpa armigera* nucleopolyhedrovirus budded virus production and occlusion body assembling. Sci Rep 5:11088

Yu H, He L, Ou-Yang YY, Huang GH (2018a) Preparation and molecular characterization of a polyclonal antibody as an efficient cutworm reference protein. J Asia Pac Entomol 21:786–792

Yu H, Li ZQ, He L, Ou-Yang YY, Ni L, Huang GH (2018b) Response analysis of host *Spodoptera exigua* larvae to infection by *Heliothis virescens ascovirus* 3 h (HvAV-3h) via transcriptome. Sci Rep 8:5367

Zhang H, Zhang YA, Qin QL, Li X, Miao L, Wang YZ, Qu LJ, Zhang AJ, Yang Q (2009) A cell strain cloned from *Spodoptera exigua* cell line (IOZCAS-Spex-II) highly susceptible to S. exigua nucleopolyhedrovirus infection. In Vitro Cell Dev Biol Anim 45: 201–204

Zhu SM, Wang W, Wang Y, Yuan MJ, Yang K (2013) The baculovirus core gene ac83 is required for nucleocapsid assembly and per os infectivity of Autographa californica nucleopolyhedrovirus. J Virol 87:10573–10586